4to Congreso Internacional, 2do Congreso Nacional de Métodos Numéricos en Ingeniería y Ciencias Aplicadas
M.C. Súarez, S. Gallegos, F. Zárate, S. Botello, M. Moreles, J. Perez y F. Domínguez (Editores)

COMPUTATION OF A MODEL OF LAMINATES WITH INTERLAMINAR DAMAGE

G. Aquino, R. Castañeda, A. Díaz
Centro de Investigación en Materiales Avanzados
(CIMAV)
Miguel de Cervantes 120, Compl. Ind. Chih.
31109 Chihuahua, Chih. México
Email: alberto.diaz@cimav.edu.mx,
web page: http://www.cimav.edu.mx

Abstract. In this paper, a model of laminated plates called M4-5N and validated in a previous paper is modified in order to take into account damage at the interfaces between layers. Displacement discontinuities at the interfaces are considered in the model. These discontinuities are calculated by means of a damage model. This damage model involves non linear equations. In order to compute the model, the LATIN method is employed. With this method, two sub-problems are considered: one is linear and the other is non linear. In the linear problem the non-linear equations of the model are linearized. By iterating the resolution of each sub-problem, one obtains the solution of the global problem. The method is then applied to the resolution of a free edge problem of a composite laminate. Calculations prove that the model can help predict delamination in these laminates.

Keywords: laminates, interlaminar damage, model, algorithm, delamination.

1 INTRODUCTION

Delamination is perhaps the most critical failure mode in laminated structures. It is generally due to the stress concentration near the edges at the interfaces between layers. Thus, it is necessary to calculate the edge effects on the interlaminar stresses and to use a delamination criterion in order to predict delamination onset. In order to study delamination, a linear elastic behavior is widely assumed for stress evaluation. Besides, a more complex theory than the classical laminate theory is used because the interlaminar stresses must be calculated.

3D finite elements can be used to calculate the interlaminar stresses. Nevertheless, these stresses are often singular at the edges of the laminates and the calculations do not converge to a finite value[1]. With this calculation method, a delamination criterion must involve the singularity intensity factor or the averages of the interlaminar stresses over a characteristic distance from the edge[1,2]. Another calculation method is the asymptotic expansion technique which can be applied in order to calculate the interlaminar stresses. The software CLEOPS developed by Lécuyer[3] uses this last technique. Other authors use models of laminated plates[2,4] which provide finite stress values and are easier to handle than the 3D calculations. One example of

these models is the M4-5N model[4,5] (Multi-particle Model of Multi-layered Materials with 5 kinematic fields per layer for an N layer laminate) implemented in the software called DEILAM developed by Díaz et al[6]. The approximate stresses of this model are finite even at the edges and the maximum values of stresses can be then considered in the delamination criterion expression[7]. The M4-5N model is similar to Pagano's local model[8]. Its equations are obtained by adapting the Hellinger-Reissner variational formulation[9]. The M4-5N model has already been validated for thermal elastic problems[7].

Even if the linear elastic assumption is commonly used, non linear phenomena appear at the interfaces[10], especially for composite materials with polymeric matrixes. Díaz and Caron[7] observed that microcracks appear at the interfaces long time before delamination initiates. When these microcracks coalesce, a macrocrack like delamination takes place. This phenomenon can be modeled by means of a continuum damage mechanics model[11].

In this paper, the interlaminar damage is calculated by adapting and introducing a damage model into the M4-5N model. The laminate is supposed to be made up of linear elastic layers and damageable interfaces. The LATIN method[12] is then applied for the numerical resolution. Finally two application examples are considered.

Notations

Throughout this work,

- superscripts *i* and *j,j+1* indicate layer *i* and the interface between layers *j* and *j+1* ($1 \le i \le N$, $1 \le j \le N-1$), respectively,
- subscripts ",1", ",2" and ",3" denote the partial derivatives with respect to *x*, *y* and *z*, respectively
- bold face characters define tensors, matrices and vectors
- the multi-layer lies within the volume defined by $\begin{cases} (x,y) \in \omega \\ z \in \left[h_-^1, h_+^N\right] \end{cases}$;
- layer *i* occupies the geometrical space defined by $\begin{cases} (x,y) \in \omega \\ z \in \left[h_-^i, h_+^i\right] \end{cases}$; its thickness is $t^i = h_+^i - h_-^i$,
- subscripts *o*, *p*, *q* and *r* indicate the components in the (x,y,z) space; they are assigned the values 1, 2 and 3,
- subscripts α, β, γ and δ indicate the components on the (x,y) plane and are assigned the values 1 and 2,
- $\mathbf{U}$ and $\boldsymbol{\sigma}$ denote respectively the 3D displacement field and the 3D stress field,
- $\Gamma^{j,j+1}$ denotes the interface between layers *j* and *j*+1,
- $\boldsymbol{\gamma}^{j,j+1}$ denotes the first order tensor of displacement discontinuities at the interface $\Gamma^{j,j+1}$ defined by the following equation:

$$\lim_{z \xrightarrow{>} h_+^k} U_o(x,y,z) - \lim_{z \xrightarrow{<} h_+^k} U_o(x,y,z) = \gamma_o^{k,k+1}(x,y) \qquad (1)$$

- each layer *i* is orthotropic and the orthotropy directions are L_i, T_i and N_i as defined by the vectors $\mathbf{e}_{L_i} = \cos\theta_i \mathbf{e}_x + \sin\theta_i \mathbf{e}_y$, $\mathbf{e}_{T_i} = \sin\theta_i \mathbf{e}_x + \cos\theta_i \mathbf{e}_y$ and $\mathbf{e}_{N_i} = \mathbf{e}_z$
- $\mathbf{S}(x,y,z) = \mathbf{S}(z)$ denotes the 4th-order tensor of compliances; it is constant in each layer. Its components are S_{opqr}, with $S_{opqr} = 0$ in the presence of an odd number of 3 (*z*-direction) in the set *opqr*,
- the second-order tensors $\mathbf{S^i}$ and $\mathbf{S_Q^i}$ represent the in-plane and shearing compliances of layer *i*, respectively; they are defined by:

$S^i_{\alpha\beta} = S_{\alpha\alpha\beta\beta}(z)$, $S^i_{16} = S^i_{61} = 2S_{1112}(z)$, $S^i_{26} = S^i_{62} = 2S_{2212}(z)$, $S^i_{66} = 4S_{1212}(z)$, $S^i_{Q\,\alpha\beta} = 4S_{\alpha 3\beta 3}(z)$ for $z \in \left[h^i_-, h^i_+\right]$. The scalar S^i_3 denotes the normal compliance of layer *i* and is defined by: $S^i_3 = S_{3333}(z)$ for $z \in \left[h^i_-, h^i_+\right]$.

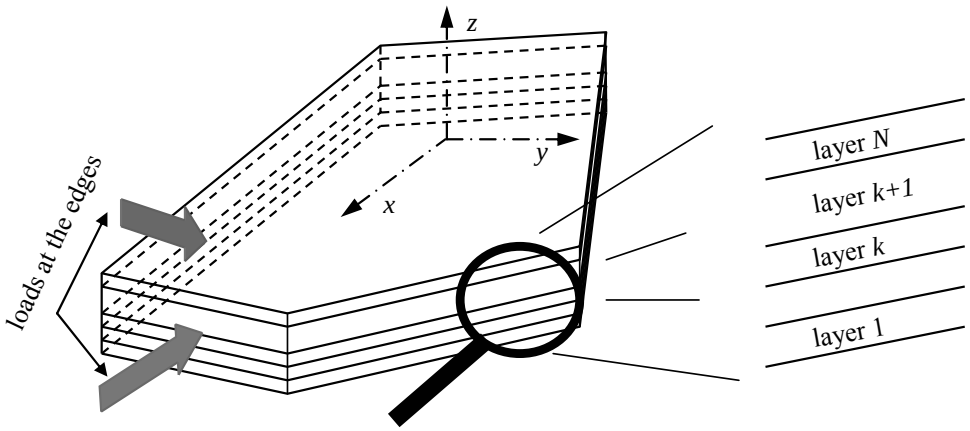

Figure 1 – Considered laminate

2 MODEL EQUATIONS

By using the *M4-5N* model, the multi-layer (3-D object) becomes a superposition of *N* Reissner plates[13] (a 2-D object with *N* particles at each geometrical point and for each particle 5 kinematic fields are considered) coupled with interlaminar stresses. This model has been inspired by Pagano's work[8] and already developed and validated in its linear elastic version[4,6]. The model[5,6] takes into account displacement discontinuities at the interfaces between layers; these fields are supposed to be known. Since these discontinuity fields are given data, the constitutive equations of the model are linear elastic. Herein, the interface is modelled as a thin layer within which damage may occur and the displacement discontinuities depend on the amount of damage in the interface. The damage model chosen in this paper contains non linear equations and it is inspired by that employed by Allix and Blanchard[10].

Since the linear elastic equations of the model have already been developed, in this section the authors make a brief review. The model is obtained by means of adapting[5,6] the classical Hellinger-Reissner formulation of 3-D elastic problems[9] and choosing approximate stresses. The formulation yields approximate displacements, which are consistent with the stress approximation and are discontinuous at the cracked interface as desired. Using the variational properties of the formulation, we obtain the equations of the model.

The M4-5N model (linear version)

The in-plane stress components $\sigma_{\alpha\beta}$ $(\alpha,\beta \in \{1,2\})$ are chosen as linear functions of z and the 3D equilibrium equations lead both to shear stresses $\sigma_{\alpha 3}$ in the form of quadratic polynomials of z and to the normal stress σ_{33} as third-order polynomials. The polynomial coefficients are expressed in terms of the following generalized internal forces[4,5,6]:

- force, moment and shear resultants of layer *i*, respectively :

$$N^i_{\alpha\beta}(x,y) = \int_{h^i_-}^{h^i_+} \sigma_{\alpha\beta}(x,y,z)\,dz\,,\; M^i_{\alpha\beta}(x,y) = \int_{h^i_-}^{h^i_+} \left(z - \overline{h}^i\right)\sigma_{\alpha\beta}(x,y,z)\,dz \qquad (2)$$

$$\text{and } Q_\alpha^i(x,y) = \int_{h_-^i}^{h_+^i} \sigma_{\alpha 3}(x,y,z)\,dz$$

where $\bar{h}^i = \dfrac{h_+^i + h_-^i}{2}$

- interfacial shear and normal stresses at interfaces $\Gamma^{j,j+1}$:

$$\tau_\alpha^{j,j+1}(x,y) = \sigma_{\alpha 3}(x,y,h_+^j)\,,\ \nu^{j,j+1}(x,y) = \sigma_{33}(x,y,h_+^j) \tag{3}$$

where $(x,y) \in \omega$.

Once the approximate stresses are defined, the Hellinger-Reissner formulation helps to identify

- the following $5N$ generalized displacements for $(x,y) \in \omega$:

$$U_\alpha^i(x,y) = \int_{h_-^i}^{h_+^i} \frac{1}{t^i} U_\alpha(x,y,z)dz\,,\ \Phi_\alpha^i(x,y) = \int_{h_-^i}^{h_+^i} \frac{12\,(z-\bar{h}^i)}{t^{i\,3}} U_\alpha(x,y,z)dz\,, \tag{4}$$

$$U_3^i(x,y) = \int_{h_-^i}^{h_+^i} \frac{1}{t^i} U_3(x,y,z)dz$$

- the following generalized strains for $(x,y) \in \omega$:

$$\varepsilon_{\alpha\beta}^i(x,y) = \frac{1}{2}\left(U_{\alpha,\beta}^i + U_{\beta,\alpha}^i\right),\ \chi_{\alpha\beta}^i(x,y) = \frac{1}{2}\left(\Phi_{\alpha,\beta}^i + \Phi_{\beta,\alpha}^i\right), \tag{5}$$

$$d_{\Phi\,\alpha}^i(x,y) = \Phi_\alpha^i + U_{3,\alpha}^i\,,\ D_\alpha^{j,j+1}(x,y) = U_\alpha^{j+1} - U_\alpha^j - \frac{t^j}{2}\Phi_\alpha^j - \frac{t^{j+1}}{2}\Phi_\alpha^{j+1},$$

$$\text{and } D_3^{j,j+1}(x,y) = U_3^{j+1} - U_3^j$$

- the generalized displacement discontinuities at the interfaces for $(x,y) \in \omega$:

$$\gamma_\alpha^{j,j+1}(x,y) \text{ and } \gamma_3^{j,j+1}(x,y) \tag{6}$$

Using the variational properties[9] of the formulation for a variation of the 3D displacements and consequently of the generalized displacements, one obtains the generalized $5N$ equilibrium equations and the generalized boundary conditions at the edges[4,5,6]. Lastly, in applying equations (5) and (6) and the variational properties of the formulation for a variation of the approximate stresses, one obtains the generalized elastic constitutive equations[4,5,6] related to:

- the in-plane force resultants in layer i ($1 \le i \le N$):

$$\varepsilon_{\alpha\beta}^i = \frac{S_{\alpha\beta\gamma\delta}^i}{t^i} N_{\gamma\delta}^i \tag{7}$$

- the in-plane moment resultants in layer i ($1 \le i \le N$):

$$\chi_{\alpha\beta}^i = \frac{12}{t^{i\,3}} S_{\alpha\beta\gamma\delta}^i M_{\gamma\delta}^i \tag{8}$$

- the out-of-plane shear resultants in layer i ($1 \le i \le N$):

$$d^i_{\Phi\,\alpha} = \frac{6}{5t^i} S^i_{Q\,\alpha\beta} Q^i_\beta - \frac{1}{10} S^i_{Q\,\alpha\beta} \left(\tau^{i,i+1}_\beta + \tau^{i-1,i}_\beta \right) \tag{9}$$

- the shear stresses at interface $\Gamma^{j,j+1}$ $(1 \le j \le N-1)$

$$\begin{aligned} D^{j,j+1}_\alpha - \gamma^{j,j+1}_\alpha = & -\frac{1}{10} S^j_{Q\alpha\beta} Q^j_\beta - \frac{1}{10} S^{j+1}_{Q\alpha\beta} Q^{j+1}_\beta - \frac{t^j}{30} S^j_{Q\alpha\beta} \tau^{j-1,j}_\beta \\ & + \frac{2}{15} \left(t^j S^j_{Q\alpha\beta} + t^{j+1} S^{j+1}_{Q\alpha\beta} \right) \tau^{j,j+1}_\beta - \frac{t^{j+1}}{30} S^{j+1}_{Q\alpha\beta} \tau^{j,j+1}_\beta \end{aligned} \tag{10}$$

- the normal stresses at interface $\Gamma^{j,j+1}$ $(1 \le j \le N-1)$

$$\begin{aligned} D^{j,j+1}_3 - \gamma^{j,j+1}_3 = & \frac{9}{70} t^j S^j_3 \nu^{j-1,j} + \frac{13}{35} \left(t^j S^j_3 + t^{j+1} S^{j+1}_3 \right) \nu^{j,j+1} \\ & + \frac{9}{70} t^{j+1} S^{j+1}_3 \nu^{j+1,j+2} \end{aligned} \tag{11}$$

where $\tau^{0,1}_\alpha(x,y) = -T^d_\alpha(x,y,h^1_-)$, $\tau^{N,N+1}_\alpha(x,y) = T^d_\alpha(x,y,h^N_+)$, $\nu^{0,1}(x,y) = -T^d_3(x,y,h^1_-)$, $\nu^{N,N+1}(x,y) = T^d_3(x,y,h^N_+)$ and $\gamma^{j,j+1}_\alpha = \gamma^{j,j+1}_3 = 0$ if $j \neq k$. $\mathbf{T}^d$ denotes the external surfacic force at the upper and lower faces of the multi-layer.

The model equations being recalled, the interfacial stresses can be determined in the laminate for given displacement discontinuity fields $\boldsymbol{\gamma}^{j,j+1}$. These fields are still unknown but in the next subsection they will be determined.

Interlaminar damage model

The interfaces between layers are modelled by thin layers (e mm thick). In these "interface layers" the 3D strain $\varepsilon^{j,j+1}_{op}$ and stress $\sigma^{j,j+1}_{op}$ fields are approximated by (x,y) fields that do not depend on z (this is justified by the small thickness of the interface). Thus, the displacement discontinuities are:

$$\gamma^{j,j+1}_1 = 2e\varepsilon^{j,j+1}_{13},\ \gamma^{j,j+1}_2 = 2e\varepsilon^{j,j+1}_{23} \text{ and } \gamma^{j,j+1}_1 = e\varepsilon^{j,j+1}_{33}. \tag{12}$$

In the "interface layers" an isotropic linear elastic damageable material is considered. Its 3D constitutive equations provide:

$$\begin{aligned} \gamma^{j,j+1}_1(x,y) &= 2e\,\tau^{j,j+1}_1(x,y) \frac{(1+\nu^0)}{E^0(1-d^{j,j+1}(x,y))} \\ \gamma^{j,j+1}_2(x,y) &= 2e\,\tau^{j,j+1}_2(x,y) \frac{(1+\nu^0)}{E^0(1-d^{j,j+1}(x,y))} \\ \gamma^{j,j+1}_3(x,y) &= \begin{cases} e\,\nu^{j,j+1}(x,y) \dfrac{(1+\nu^0)}{E^0(1-d^{j,j+1}(x,y))} & \text{if } \nu^{j,j+1} > 0 \\ e\,\nu^{j,j+1}(x,y) \dfrac{(1+\nu^0)}{E^0} & \text{if } \nu^{j,j+1} \le 0 \end{cases} \end{aligned} \tag{13}$$

where E^0 and ν^0 denote the Young's modulus and Poisson's ratio of the undamaged material, $d^{j,j+1}$ denotes the damage parameter of interface $\Gamma^{j,j+1}$ (if $d^{j,j+1} = 0$ no damage exists, if $d^{j,j+1} = 1$ a delamination crack appears). The damage parameter represents the homogenized volume fraction of microcracks at a point in the interface. This parameter is calculated by the equations of classical continuum damage mechanics[11]:

$$\begin{cases} Y = \dfrac{\left(1+\nu^0\right)\left(\tau_1^{j,j+1}\right)^2}{E^0\left(1-d^{j,j+1}\right)^2} + \dfrac{\left(1+\nu^0\right)\left(\tau_2^{j,j+1}\right)^2}{E^0\left(1-d^{j,j+1}\right)^2} + \delta(\nu^{j,j+1})\dfrac{\left(\nu^{j,j+1}\right)^2}{2E^0\left(1-d^{j,j+1}\right)^2} \\ d^{j,j+1} = \sup_{\tau\le t}\left(\dfrac{\sqrt{Y}-\sqrt{Y_0}}{\sqrt{Y_c}},0\right) \end{cases} \tag{14}$$

where Y_0 and Y_c are material constants, $\delta(\nu^{j,j+1}) = 1$ if the interlaminar normal stress is positive or else it is zero, $\sup_{\tau\le t}(f,g)$ is the maximum value of f and g until the actual instant t. The material constant Y_0 defines the moment when the interlaminar stresses can initiate interlaminar damage. A small Y_0/Y_c ratio provokes a quick damage growth. With the model equations in the previous sub-section and equations (13) and (14), the displacement discontinuities can be determined for the given loads applied at the boundaries of the laminate.

3 NUMERICAL RESOLUTION AND ALGORITHM

The laminate is subjected at its boundaries to a mechanical load. Before reaching its value, the mechanical load takes intermediate values called load steps. In order to solve the equations for each load step, the LATIN (LArge Time Increment) method developed by Allix and Vidal[12] is applied. The linear equations and the non linear equations are separated. Two sub-problems are then considered: the first is non linear (problem A) and the other is linear (problem B).

In problem A, a provisional solution of problem A $\mathfrak{s}_n = (\tilde{d}_n^{j,j+1}, \tilde{\gamma}_n^{j,j+1}, \tilde{\tau}_{\alpha,n}^{j,j+1}, \tilde{\nu}_n^{j,j+1})$ is transformed into a new provisional and more accurate solution $\hat{s} = (\hat{d}^{j,j+1}, \hat{\gamma}^{j,j+1}, \hat{\tau}_\alpha^{j,j+1}, \hat{\nu}^{j,j+1})$ by means of the following equations which are deduced from equations (13) and (14):

$$\begin{cases} \hat{\tau}_1^{j,j+1} = \tilde{\tau}_{1,n}^{j,j+1}, \hat{\tau}_2^{j,j+1} = \tilde{\tau}_{2,n}^{j,j+1}, \hat{\nu}^{j,j+1} = \tilde{\nu}_n^{j,j+1}, \\ \hat{Y} = \dfrac{\left(1+\nu^0\right)\left(\tilde{\tau}_{1,n}^{j,j+1}\right)^2}{E^0\left(1-\tilde{d}_n^{j,j+1}\right)^2} + \dfrac{\left(1+\nu^0\right)\left(\tilde{\tau}_{2,n}^{j,j+1}\right)^2}{E^0\left(1-\tilde{d}_n^{j,j+1}\right)^2} + \delta(\tilde{\nu}_n^{j,j+1})\dfrac{\left(\tilde{\nu}_n^{j,j+1}\right)^2}{2E^0\left(1-\tilde{d}_n^{j,j+1}\right)^2}, \\ \hat{d}^{j,j+1} = \sup_{\tau\le t}\left(\dfrac{\sqrt{\hat{Y}}-\sqrt{Y_0}}{\sqrt{Y_c}},0\right), \\ \hat{\gamma}_\alpha^{j,j+1}(x,y) = 2e\,\hat{\tau}_\alpha^{j,j+1}(x,y)\dfrac{(1+\nu^0)}{E^0(1-\hat{d}^{j,j+1}(x,y))}, \\ \hat{\gamma}_3^{j,j+1}(x,y) = e\,\hat{\nu}^{j,j+1}(x,y)\dfrac{1}{E^0(1-\hat{d}^{j,j+1}(x,y))} \end{cases} \tag{15}$$

In problem B, the provisional solution $\hat{s} = (\hat{d}^{j,j+1}, \hat{\gamma}^{j,j+1}, \hat{\tau}_\alpha^{j,j+1}, \hat{\nu}^{j,j+1})$ of problem B is considered and a new provisional and more accurate solution $\mathfrak{s}_{n+1} = (\tilde{d}_{n+1}^{j,j+1}, \tilde{\gamma}_{n+1}^{j,j+1}, \tilde{\tau}_{\alpha,n+1}^{j,j+1}, \tilde{\nu}_{n+1}^{j,j+1})$ is calculated. In this linear problem, the non linear equations are linearized:

$$\begin{pmatrix} \tilde{\gamma}_{1,n+1}^{j,j+1} \\ \tilde{\gamma}_{2,n+1}^{j,j+1} \\ \tilde{\gamma}_{3,n+1}^{j,j+1} \end{pmatrix} = \begin{pmatrix} \hat{\gamma}_1^{j,j+1} \\ \hat{\gamma}_2^{j,j+1} \\ \hat{\gamma}_3^{j,j+1} \end{pmatrix} + \mathbf{A}\begin{pmatrix} \tilde{\tau}_{1,n+1}^{j,j+1} - \hat{\tau}_1^{j,j+1} \\ \tilde{\tau}_{2,n+1}^{j,j+1} - \hat{\tau}_2^{j,j+1} \\ \tilde{\nu}_{n+1}^{j,j+1} - \hat{\nu}^{j,j+1} \end{pmatrix} + \mathbf{a} \tag{16}$$

where **A** is a 3×3 matrix and **a** is a vector. Their coefficients are given by the linearization of $\hat{Y}(\tilde{d}^{j,j+1},\tilde{\tau}_1^{j,j+1},\tilde{\tau}_2^{j,j+1},\tilde{\nu}^{j,j+1})$, $\hat{\gamma}^{j,j+1}(\tilde{d}^{j,j+1},\tilde{\tau}_1^{j,j+1},\tilde{\tau}_2^{j,j+1},\tilde{\nu}^{j,j+1})$ and $\hat{d}^{j,j+1}(\tilde{d}^{j,j+1},\tilde{\tau}_1^{j,j+1},\tilde{\tau}_2^{j,j+1},\tilde{\nu}^{j,j+1})$ in equations (13) and (14). For example, for the A_{11} and a_1 terms one obtains:

$$A_{11}=\frac{2e(1+\nu^0)}{E^0\left(1-\hat{d}^{j,j+1}\right)} \tag{17}$$

$$a_1=\frac{2e\hat{\tau}_1^{j,j+1}(1+\nu^0)}{E^0\left(1-\hat{d}^{j,j+1}\right)^2}\times\frac{\sqrt{\dfrac{(1+\nu^0)}{E^0}\left(\left(\tilde{\tau}_{1,n}^{j,j+1}\right)^2+\left(\tilde{\tau}_{2,n}^{j,j+1}\right)^2\right)+\dfrac{\delta(\tilde{\nu}_n^{j,j+1})}{2E_0}\left(\tilde{\nu}_n^{j,j+1}\right)^2}}{\sqrt{Y_c}\left(1-\tilde{d}_n^{j,j+1}\right)^2}\left(\hat{d}^{j,j+1}-\tilde{d}_n^{j,j+1}\right) \tag{18}$$

Finally, by taking into account the generalized linear equations (equilibrium and constitutive equations, boundary conditions) and equation (16), one obtains a linear differential equation set which is solved by means of a finite element technique as proposed by Díaz et al[6].

The global problem is the calculation of the solution $s=(d^{j,j+1},\boldsymbol{\gamma}^{j,j+1},\tau_\alpha^{j,j+1},\nu^{j,j+1})$ for each load step defined by the loads applied at the boundaries of the laminate. The numerical algorithm adopted in this paper is described in figure 2. For the first load step, the given data $s=0$.

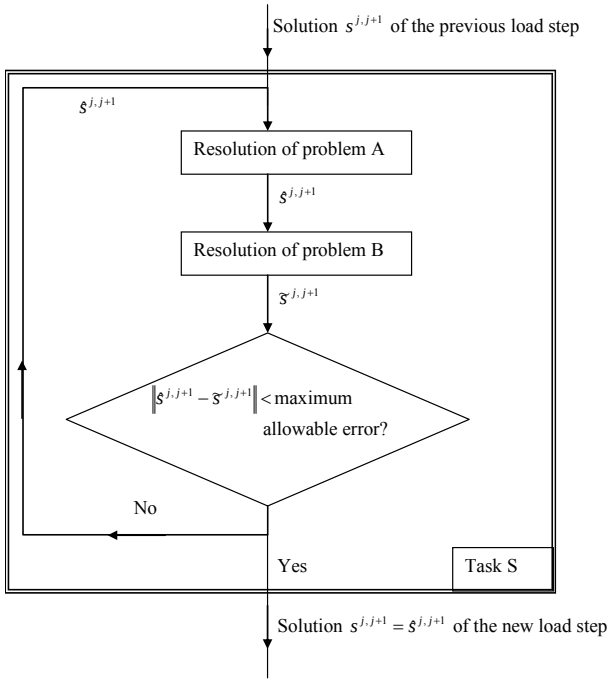

Figure 2 – Resolution of a new load step.

4 APPLICATION EXAMPLE

Let us now apply the model to the resolution of a free edge problem of a symmetrical composite laminate (see figure 3). In this problem, the laminate is made up of unidirectional composite layers and is subjected to a tensile load ε at its ends. The laminate is supposed to be infinitely long and owing to symmetries the problem can be reduced to the determination of the interlaminar damage in the shaded quarter section of this figure.

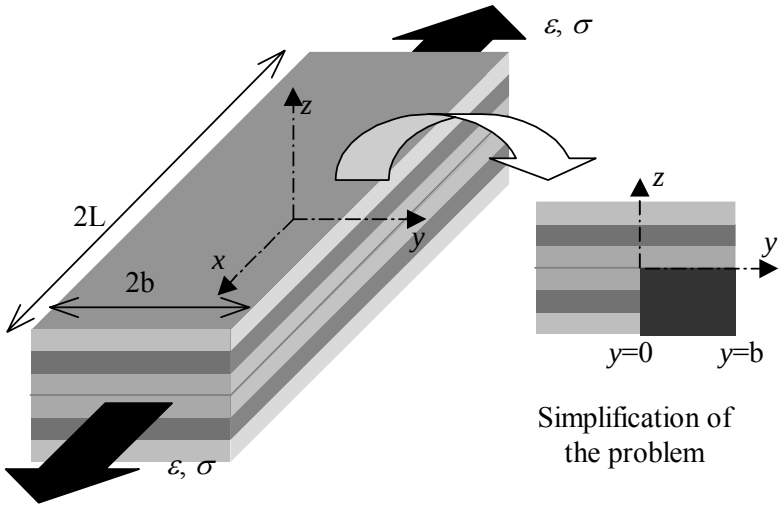

Figure 3 – Free edge problem of a symmetrical composite laminate

The material in each layer is the unidirectional carbon-epoxy composite used by Díaz and Caron[7,10]. The ply thickness is $t_p = 0.13$ mm and the ply elastic properties are:

$$E_L = 153.82\,\text{GPa},\ E_T = E_N = 10.61\,\text{GPa}$$
$$G_{LT} = G_{LN} = G_{TN} = 5.58\,\text{GPa}$$
$$\nu_{LT} = \nu_{LN} = \nu_{TN} = 0.315$$

where the subscripts L, T, N refer to the longitudinal, transverse and thickness directions of the individual ply. For the properties of the "interface layers" in these materials, a further analysis must be performed in order to identify them. In the present paper, the authors have chosen arbitrarily (except for the thickness) the following values to show the potential of the theoretical tool developed herein:

$t = 3\mu\text{m}$ (measured with an optical microscope[10])

$$E^0 = 8\text{GPa},\ \nu^0 = 0.3$$
$$Y_0 = 4.7\times10^5\,\text{Pa},\ Y_c = 4.7\times10^6\,\text{Pa}$$

Let us consider two types of laminates: $(0.90)_s$ and $(\pm10)_s$.

$(0.90)_s$ laminate

It is well known that in this laminate the interface 0/90 exhibits the largest edge effect. In figure 4, the evolution of the interlaminar shear stress $\tau_{yz}^{1,2}$ along the interface 0/90 is shown for three different load values. For the first load ($\varepsilon = 0.065$), the damage parameter is zero. An important edge effect is observed. Beyond the first load, damage appears first at the edge and propagates inside the laminate as can be seen in figure 5.

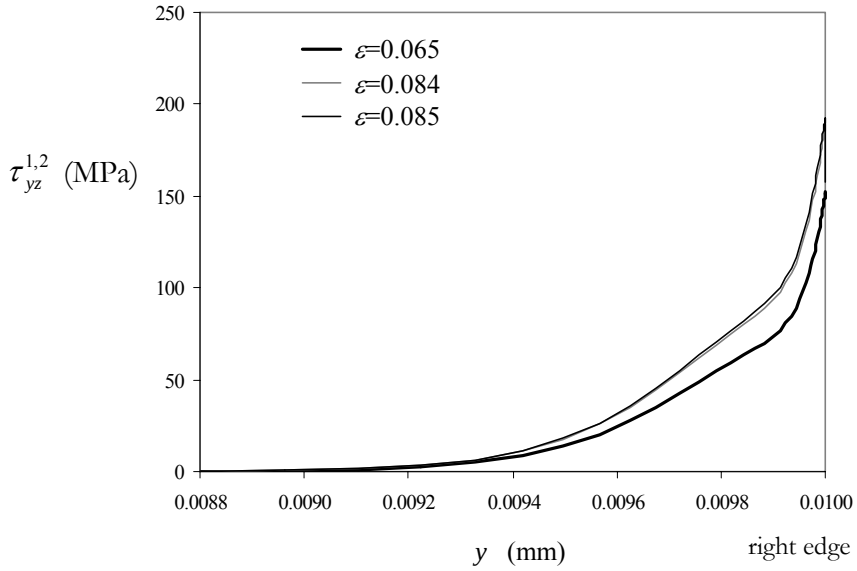

Figure 4. Interlaminar shear stress at the interface 0/90 vs. position

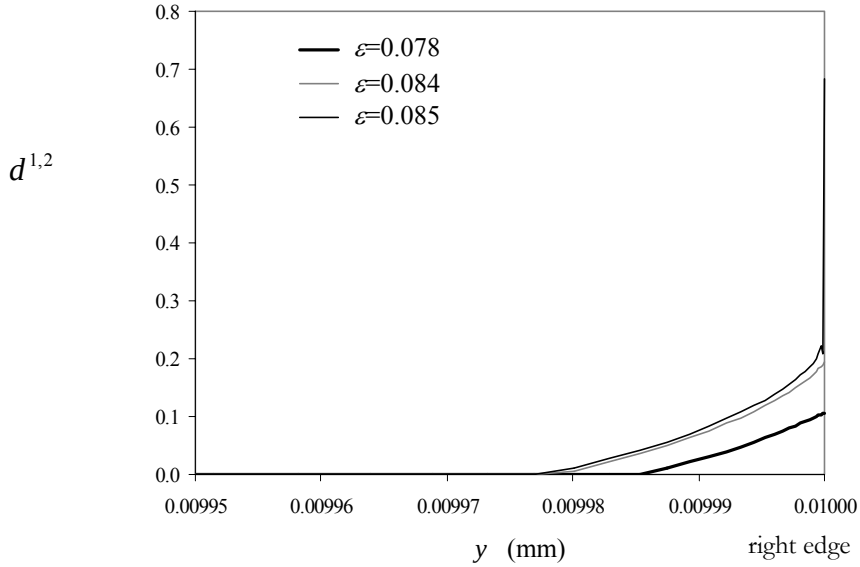

Figure 5 – Damage parameter at the 0/90 interface vs. position

Let us now analyze the edge values of the interlaminar damage and interlaminar shear stress. In figure 6, these values are plotted for different load values. Once the interlaminar damage reaches the 0.2 value, damage grows rapidly and the shear stress diminish considerably. For a $\varepsilon = 0.08505$ load, delamination appears ($d^{j,j+1} = 1$ at the edge).

With these calculations delamination onset in this laminate can be predicted. Nevertheless, in reality this laminate exhibits first intralaminar transverse cracks[13] that are not considered in the model. For the next example, delamination really appears before any other failure mode.

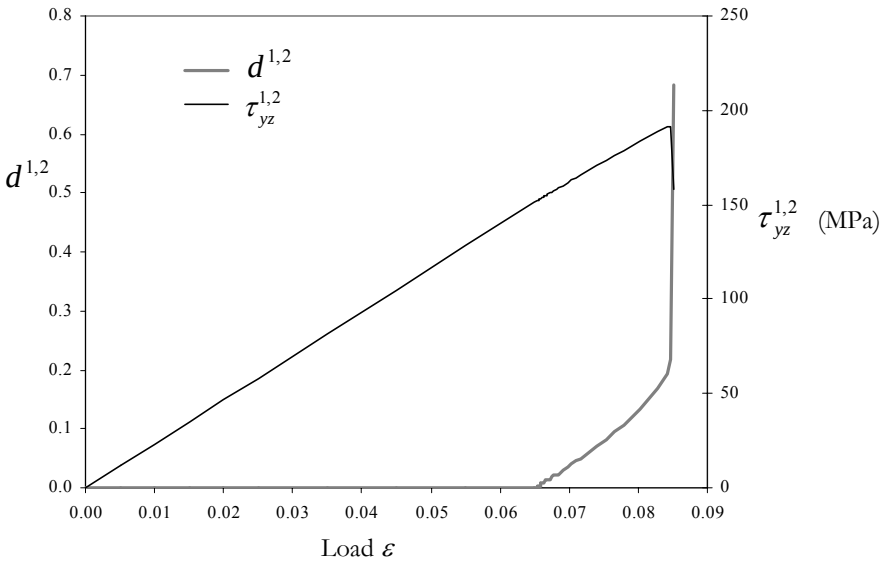

Figure 6 – Damage parameter and interlaminar shear stress at the edge vs. load

$(\pm 10_n)_s$ laminate

It is well known that mode III delaminations appear in these laminates at the 10/-10 interfaces due to the edge effect on the interlaminar stresses[1,2,7]. Besides, an important thickness effect on delamination is observed[7]: as n increases the critical tensile load that provokes delamination decreases. Let us apply our model to these laminates. Each set of n layers is modeled as a single layer ne_l thick (e_l is the ply thickness). In figure 7, the evolution of the interlaminar damage parameter at the edge is plotted for different loads. One can see that the model predicts a thickness effect on the critical load that leads to $d^{1,2}=1$ (delamination onset).

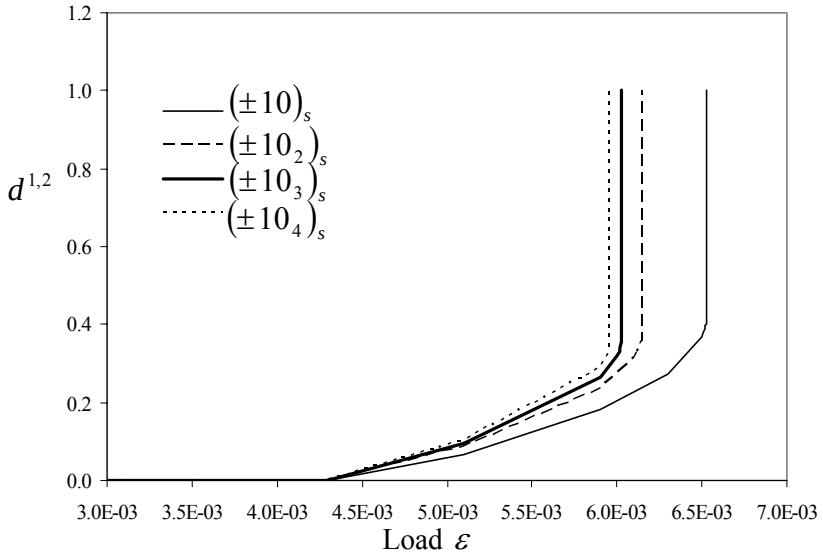

Figure 7 – Damage parameter at the edge of the 10/-10 interface vs. load

In order to compare the predictions of the model with experimental results, the interlaminar properties that appear in the model must be identified by means of a further analysis. After the achievement of this identification, the model could be validated and used for delamination onset prediction in other laminates.

5 CONCLUSION

In conclusion, a theoretical tool has been developed to calculate the interlaminar damage in laminated structures. A model of interlaminar damage has been introduced into the model of laminated plates called M4-5N. The nonlinear equations of the model are solved by means of a numerical technique based on the LATIN method. Two example applications were shown and in these examples the calculated interlaminar damage can help predict delamination onset.

The comparison of the predictions with experimental data will require an identification of the parameters that appear in the model. This comparison will help also to validate the calculations developed in this paper. After this, the new model developed in this paper may prove to be an accurate tool for delamination onset prediction in laminated structures.

6 ACKNOWLEDGEMENTS

The authors would like to acknowledge CONACYT for its financial support.

7 REFERENCES

[1] D. Leguillon, G. Marion, R. Harry, F. Lécuyer, "The onset of delamination at stress-free edges in angle-ply laminates — analysis of two criteria ", *Composites Science and Technology*, **61**, 377-382 (2001).

[2] J.C. Brewer, P.A. Lagace, "Quadratic stress criterion for initiation of delamination", *Journal of Composite Materials*, **22**, 1141-1155 (1988).

[3] F. Lécuyer. *Etude des effets de bord dans les structures minces multicouches*. PhD Thesis, Université Paris VI, France, (1991).

[4] R.P. Carreira, J.F. Caron, A. Díaz, "Model of multilayered materials for interface stresses estimation and validation by finite element calculations", *Mechanics of Materials*, **34**, 217-230 (2002).

[5] A. Díaz, J.F. Caron, R.P. Carreira, "Un modèle de stratifiés", *Comptes Rendus de l'Académie des Sciences*, **329**, 873-879 (2001).

[6] A. Díaz, J.F. Caron, R.P. Carreira, " Software application for evaluating interfacial stresses in inelastic symmetrical laminates with free edges", *Journal of Composite Structures*, **58**, 195-208 (2002).

[7] A. Díaz, JF. Caron, "Prediction of the onset of mode III delamination in carbon-epoxy laminates", *Journal of Composite Structures*, **72**, 438-445 (2006).

[8] N.J. Pagano, "Stress fields in composite laminates", *International Journal of Solids and Structures*, **14**, 385-400 (1978).

[9] E. Reissner, "On a variational theorem in elasticity", *Journal of Mathematics and Physics*, **29**, 90-95 (1950).

[10] A. Díaz, J.F. Caron, "Interface plasticity and delamination onset prediction", *Mechanics of Materials*, **38**, 648-663 (2006).

[11] O. Allix, L. Blanchard, "Mesomodeling of delamination: towards industrial applications", *Composites Science and Technology*, **66**, 731-744 (2006).

[12] O. Allix, P. Vidal, "A new multi-solution approach suitable for structural identification problems", *Computer Methods in Applied Mechanics and Engineering*, **191**, 2727-2758 (2002).

[13] E. Reissner, "The effect of transverse shear deformation on the bending of elastic plates", *Journal of Applied Mechanics*, **A**, 69-77 (1945).